Dental Materials Journal 2017; 36(1): 19–26

Effect of mechanochemical surface preparation on bonding to zirconia of a tri-*n*-butylborane initiated resin

Nobutaka AKAZAWA[1], Hiroyasu KOIZUMI[2,3], Hiroshi NOGAWA[2], Daisuke NAKAYAMA[2,3], Akihisa KODAIRA[1] and Hideo MATSUMURA[2,3]

[1] *Division of Applied Oral Sciences, Nihon University Graduate School of Dentistry, 1-8-13, Kanda-Surugadai, Chiyoda-ku, Tokyo 101-8310, Japan*
[2] *Department of Fixed Prosthodontics, Nihon University School of Dentistry, 1-8-13, Kanda-Surugadai, Chiyoda-ku, Tokyo 101-8310, Japan*
[3] *Division of Advanced Dental Treatment, Dental Research Center, Nihon University School of Dentistry, 1-8-13, Kanda-Surugadai, Chiyoda-ku, Tokyo 101-8310, Japan*
Corresponding author, Hiroyasu KOIZUMI; E-mail: Koizumi.Hiroyasu@nihon-u.ac.jp

This study aimed to evaluate the effect of surface preparation on bond strength of a tri-*n*-butylborane initiated resin (MMA-TBB) bonded to zirconia. Zirconia disks were either airborne-particle abraded with alumina or silica-coated. The disks were thereafter primed with one of the following materials: phosphate-silane (Clearfil Ceramic Primer), phosphate (Alloy Primer), or silane (ESPE Sil). The specimens were bonded with the MMA-TBB. Shear bond strength was determined both before and after thermocycling. Bond strength of unprimed zirconia (control) was not affected by the surface roughness of each adherend. Priming with phosphate was effective for bonding alumina-blasted zirconia. Priming with silane was effective for bonding silica-coated zirconia. Priming effect of the phosphate-silane was superior to that of silane alone for bonding silica-coated zirconia. Bond strength to zirconia of the MMA-TBB is significantly influenced by a combination of the specific functional monomer and the surface modification performed rather than the material surface roughness.

Keywords: Bonding durability, Phosphate, Silane, Tri-*n*-butylborane, Zirconia

INTRODUCTION

Modern dentistry requires increasingly esthetic, tough, and biocompatible restorative materials. The application of ceramic materials in fixed dental prostheses and restorations have become increasingly popular because they mimic natural tooth color in comparison to other restorative materials. Zirconium oxide (zirconia) demonstrates superior mechanical properties, chemical stability, and biocompatibility compared to other ceramic materials being applied in framework structures[1,2].

Etching with hydrofluoric acid and silanization are effective methods to bond silica-based ceramic materials[3,4]. However, etching with hydrofluoric acid or silanization have no positive effect on the properties of zirconia because of their resistance to acids and absence of silicon oxide[5]. Researchers have therefore proposed a number of surface conditioning methods to achieve reliable and durable bonding to zirconia over the past two decades. The representative materials and methods are airborne-particle abrasion with aluminum oxide particles (alumina blasting)[6-12], airborne-particle abrasion with aluminum oxide modified with silica (silica-coating) followed by silanization[6,7,10,13], primers containing 10-methacryloyloxydecyl dihydrogen phosphate (MDP)[7-16], luting agents containing MDP[6,8-10,12,13], selective infiltration-etching[17], and coating with nano-structured alumina[18].

It is generally known that the inclusion of a divalent phosphoric group within the MDP monomer chemically bonds with the zirconia surface, which can improve the bond strength of resin-based luting agents to zirconia[6-16]. The bond strength to zirconia through the application of MDP alone, without mechanical retention, is not particularly excellent[9,11,12].

The use of alumina blasting to mechanically prepare zirconia prior to chemical treatment is currently recommended for the improvement in the bonding durability to zirconia. Preparation with alumina blasting increases the bonding surface area, which enhances the mechanical retention and consequently improves the effectiveness of the chemical treatment with luting agents[9,11,12]. Silica-coatings have been introduced as an alternative to abrasion with alumina. In this process, the zirconia surface is coated with silicates or silicon oxides and can consequently undergo silanization[7]. It is known that two mechanochemical surface preparations have been effective to zirconia surface. However, there is limited information of whether alumina blasting and silica-coating whichever are more superior bonding durability to zirconia.

The purpose of the current study was to evaluate the effect of mechanochemical surface preparation on the bond strength of a self-polymerizing acrylic resin bonded to zirconia.

The null hypotheses were that the type of mechanochemical (combination of airborne-particle abrasion and primer treatment) surface preparation had no difference on the bond strength obtained after thermocycling.

Color figures can be viewed in the online issue, which is available at J-STAGE.

Received Mar 14, 2016: Accepted Aug 1, 2016
doi:10.4012/dmj.2016-099 JOI JST.JSTAGE/dmj/2016-099

MATERIALS AND METHODS

Materials

The materials assessed are listed in Table 1. Disk specimens (11.4 mm in diameter and 2.8 mm thick) were fabricated with yttrium-oxide-partially-stabilized zirconia ceramics (Katana, Kuraray Noritake Dental, Tokyo, Japan) and were used as the bonding substrate.

Three abrasive particles were used for airborne-particle abrasions: 50–70 μm alumina (Hi-Aluminas, Shofu, Kyoto, Japan), 110 μm alumina (Rocatec Pre, 3M ESPE Dental Products, St. Paul, MN, USA), and 110 μm alumina modified with silica (Rocatec Plus, 3M ESPE Dental Products). Hi-Aluminas and Rocatec Pre were employed to clean and roughen the surface of the specimens. Rocatec Plus was used to coat the surface of the specimens with silica.

Three single liquid priming agents were used: Clearfil Ceramic Primer (CP, Kuraray Noritake Dental), Alloy Primer (AP, Kuraray Noritake Dental), and ESPE Sil (ES, 3M ESPE Dental Products). The priming agents used contain functional monomers: the CP contains MDP and 3-trimethoxysilylpropyl methacrylate (MPTS), whereas the AP contains MDP and 6-(4-vinylbenzyl-*n*-propyl)amino-1,3,5-triazine-2,4-dithione, -dithiol tautomer (VTD), and the ES contains MPTS.

A self-polymerizing resin consisting of a tri-*n*-butylborane (TBB) initiator (Super-Bond Catalyst V, Sun Medical, Moriyama, Japan), methyl methacrylate (MMA, Tokyo Chemical Industry, Tokyo, Japan), and poly(methyl methacrylate) (PMMA, Super-Bond Opaque Ivory powder, Sun Medical) was employed as a luting agent.

Specimen preparation and shear bond strength

Figure 1 shows the specimen preparation procedure. A total of 176 zirconia disks were wet-ground with 800-grit silicon carbide abrasive paper (Wet or Dry Tri-M-ite, 3M, St. Paul, MN, USA), cleaned with acetone for 10 min in an ultrasonic bath (SUC-110, Shofu), and then air-dried in a vacuum desiccator.

Zirconia disks were randomly divided into two groups (n=88) according to the blasting method. The group Hi-Aluminas (HAL) included the specimens that were airborne-particle abraded with 50–70 μm alumina

Table 1 Materials assessed

Material/Trade name (Abbr.)	Manufacturer	Lot No.	Composition (%)
Adherend material			
Katana Zirconia	Kuraray Noritake Dental, Tokyo, Japan	200218	ZrO_2 94.4%, Y_2O_3 5.4%
Particle abrasive			
Hi-Aluminas (HAL)	Shofu, Kyoto, Japan	031401	50–70 μm alumina particles
Rocatec Pre	3M ESPE Dental Products, St. Paul, MN, USA	207285	110 μm alumina particles
Rocatec Plus (ROC)	3M ESPE Dental Products	536184	110 μm alumina particles modified with silica
Primer			
Clearfil Ceramic Primer (CP)	Kuraray Noritake Dental	250005	MDP, MPTS, Ethanol
Alloy Primer (AP)	Kuraray Noritake Dental	190025	MDP, VTD, Acetone
ESPE Sil (ES)	3M ESPE Dental Products	532902	MPTS, Methyl ethyl ketone, Ethanol
Luting material			
MMA	Tokyo Chemical Industry, Tokyo, Japan	ZJ3WJIJ	MMA 99.8%
Super-Bond Opaque Ivory powder	Sun Medical, Moriyama, Japan	GT1	PolyMMA, titanium oxide
Super-Bond Catalyst V	Sun Medical	GG21F	TBB, TBB-O, hydrocarbon

MDP, 10-methacryloyloxydecyl dihydrogen phosphate; MPTS, 3-trimethoxysilylpropyl methacrylate;
VTD, 6-(4-vinylbenzyl-*n*-propyl)amino-1,3,5-triazine-2,4-dithione, -ditiol tautomer;
MMA, methyl methacrylate; TBB, tri-*n*-butylborane; TBB-O, partially oxidized tri-*n*-butylborane

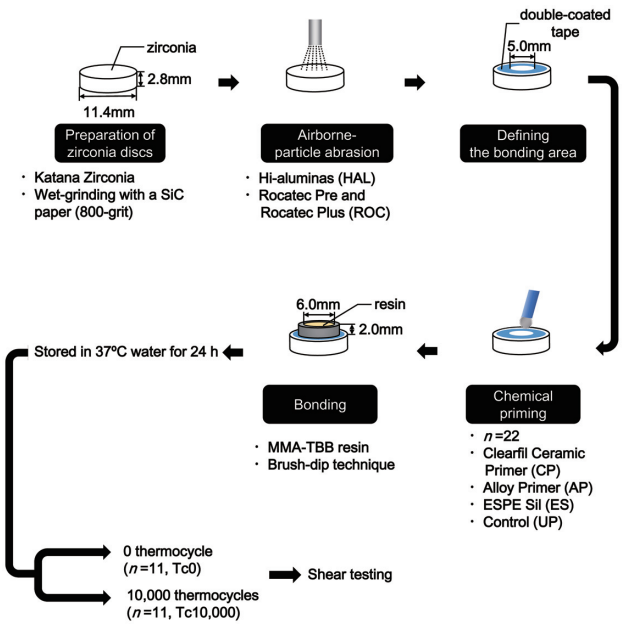

Fig. 1 Specimen preparation procedure for shear bond testing.

particles for 10 s at a 0.28 MPa air-pressure. The distance between the orifice and the disk surface was 20 mm. The bonding surface was then cleaned using compressed air for 15 s. The group Rocatec system (ROC) included the specimens that were airborne-particle abraded with 110 μm alumina particles from a distance of 20 mm for 10 s at 0.28 MPa followed by abrasion with 110 μm silica modified alumina particles (silica-coating) from a distance of 10 mm for 13 s at 0.28 MPa. The bonding surface was then cleaned using compressed air for 15 s.

A piece of double-coated tape with a circular hole, 5 mm in diameter, was placed on the disk surface to define the bonding area. The specimens were randomly divided into four subgroups (n=22): three priming agents and an unprimed control (UP). The disk specimens, with the exception of the control specimens, were subjected to one of the three priming agents according to the manufacturer's instructions. CP was applied to the zirconia surface and air-dried. AP was applied to the zirconia surface and dried under ambient conditions. ES was applied to the zirconia surface and dried for 5 min under ambient conditions.

A stainless steel ring (SUS303), which was 6 mm in inner diameter, 2 mm in height, and a 1 mm thick wall, was placed around the 5 mm diameter circular hole. The ring was filled with the MMA-TBB resin using a brush-dip technique.

After 30 min of bonding preparation, all specimens were stored in a distilled water bath at 37ºC for 24 h. This state was defined as the 0 thermocycle (Tc0), and half of the specimens (eight sets of 11 pairs) were tested at this stage. The remaining of the specimens (eight sets of 11 pairs) were thermocycled in water at a temperature between 5 and 55ºC with a 60 s dwell time per bath for 10,000 cycles (Tc10,000, Thermal Shock Tester TTS-1 LM, Thomas Kagaku, Tokyo, Japan). The specimens were fixed in a steel mold and seated in a bond test jig. The shear bond strength was recorded with a mechanical testing device (Type 5567, Instron, Caton, MA, USA) at a crosshead speed of 0.5 mm/min.

Failure mode analysis

The debonded surfaces of the specimens were observed using an optical microscope (57×, SZX9, Olympus, Tokyo, Japan) to assess the failure mode. The debonded surface were assigned into two classifications: A, adhesive failure at the luting agent/adherend interface; and CA, a combination of adhesive and cohesive failures. Cohesive failure ratios were calculated using an image-analysis application (LMeye, Lasertec, Yokohama, Japan). Cohesive failure ratio is calculated as follows:

Cohesive failure ratio (%)=Cohesive failure area (mm^2)/Adhesive area (19.63 mm^2)×100

Scanning electron microscopy observations

The specimens selected for scanning electron microscopy (SEM) observation from those submitted to the surface preparation and from those debonded after the shear bond strength test. The specimens were dried in a vacuum desiccator and sputtered with osmium (HPC-1S, Vacuum Device, Mito, Japan) for 30 s. The surfaces of the specimens were then observed using a SEM (S-4300, Hitachi High-Technologies, Tokyo, Japan) operated at 15 kV.

Surface roughness and tomography measurements

Surface roughness of the specimens ground with an 800-grit silicon carbide abrasive paper (Control), airborne-particle abraded HAL or ROC was analyzed using a profilometer (Surfcom 1400A, Tokyo Seimitsu, Tokyo, Japan). Five samples from each of the three surface modifications were measured. Each sample was measured at five lines. The arithmetical mean deviation of the roughness profile (Ra) was measured under these conditions: cut-off value of 0.8 mm and measurement length of 4.0 mm. These are based on the Japanese Industrial Standards (JIS B 0633:2001).

The surface roughness Sa and topography of the specimens were analyzed using a confocal scanning laser microscope (1LM21W, Lasertec) equipped with a He-Ne laser light source with a wavelength of 633 nm. A magnification of 20 was adopted using the objective lens. The microscope resolution was approximately 0.03 μm. The focal depth in the Z-axis scan range was defined as 24 μm. Five samples from each of the three surface modifications were also measured. Each sample was measured at five sites scans were performed over a measuring area of 400×400 μm.

Statistical analysis

The mean, median, standard deviation, and interquartile range of the shear bond strength were

calculated. The D'Agostino and Pearson omnibus test (GraphPad Prism 6.0, GraphPad software, La Jolla, CA, USA) was primarily conducted. When the results of the D'Agostino and Pearson omnibus test did not show a normal distribution, Kruskal-Wallis test (GraphPad Prism 6.0) and Steel-Dwass multiple comparisons (Kyplot 5.0, KyensLab, Tokyo, Japan) were performed as non-parametric tests to evaluate the differences between each of the three primers and UP. The effect of the surface roughness was analyzed using the Kruskal-Wallis test (GraphPad Prism 6.0) and Steel-Dwass multiple comparisons (Kyplot 5.0). Steel-Dwass test were separately conducted each of the 0 thermocycle and 10,000 thermocycles.

The comparisons between the pre- and post-thermocycling bond strengths with identical surface preparations were analyzed using the Mann-Whitney *U* test (IBM SPSS Statistics Ver. 19, IBM, Somers, NY, USA). Some binary conditions were analyzed with the Mann-Whitney *U* test. The statistical significance level was set at α=0.05.

RESULTS

Kruskall-Wallis and Steel-Dwass multiple comparisons tests

The results of the shear bond strength and statistical analysis are summarized in Tables 2 to 4. The results

Table 2 Shear bond strength (MPa) of MMA-TBB resin joined to alumina-blasted (HAL) zirconia

	0 thermocycle			10,000 thermocycles			Post-/Pre-BS Ratio (%)	
	Mean (SD)	Median	IQR	Mean (SD)	Median	IQR		
UP	3.0 (1.4)	2.3[c]	2.0	0.4 (0.1)	0.4[f]	0.1	17.4	p<0.01*
CP	28.0 (1.0)	27.8[a]	1.4	29.8 (1.6)	29.8[d]	2.9	107.2	p<0.01*
AP	27.1 (1.1)	27.1[a]	2.0	24.2 (4.1)	25.3[e]	4.0	93.4	p<0.05*
ES	19.7 (4.1)	21.0[b]	7.6	0.4 (0.1)	0.3[f]	0.3	1.4	p<0.01*

n=11; SD, Standard deviation; IQR, interquartile range; Post-/Pre-BS ratio, Post-/Pre-thermocycling bond strength ratio (%); Steel-Dwass test were separately conducted each of the 0 thermocycle column and 10,000 thermocycles column. Identical letters indicate that the values are not significantly different (p>0.05). UP: unprimed control; *Significant difference between the pre- and post-thermocycling bond strengths (Mann-Whitney *U*-test: p<0.05)

Table 3 Shear bond strength (MPa) of MMA-TBB resin joined to Rocatec- (ROC) treated zirconia

	0 thermocycle			10,000 thermocycles			Post-/Pre-BS Ratio (%)	
	Mean (SD)	Median	IQR	Mean (SD)	Median	IQR		
UP	2.4 (0.5)	2.4[j]	0.5	0.5 (0.1)	0.5[n]	0.2	20.8	p<0.01*
CP	28.8 (0.8)	28.7[g]	1.1	29.3 (2.9)	30.3[k]	2.8	105.6	p=0.08
AP	7.9 (1.5)	8.0[i]	2.7	1.8 (0.5)	1.7[m]	0.9	21.3	p<0.01*
ES	20.5 (4.3)	20.2[h]	5.7	12.6 (2.4)	13.5[l]	3.8	66.8	p<0.01*

n=11; SD, Standard deviation; IQR, interquartile range; Post-/Pre-BS ratio, Post-/Pre-thermocycling bond strength ratio (%); Steel-Dwass test were separately conducted each of the 0 thermocycle column and 10,000 thermocycles column. Different letters indicate that the values are significantly different (p<0.05). UP: unprimed control; *Significant difference between the pre- and post-thermocycling bond strengths (Mann-Whitney *U*-test: p<0.05)

Table 4 Comparison of bond strengths between specific two groups

Thermocycled groups	p	M-W
HAL-AP *vs.* ROC-ES	p<0.01	S
HAL-AP *vs.* ROC-AP	p<0.01	S
HAL-ES *vs.* ROC-ES	p<0.01	S

M-W, Abbreviation "S" indicates that the difference between the binary conditions the post-thermocycling bond strengths is significant. (Mann-Whitney *U* test: p<0.05)

of the shear bond strength test were not normally distributed according to the D'Agostino and Pearson omnibus test (p>0.05). Therefore, the bond strength results were analyzed with the Kruskal-Wallis test and Steel-Dwass multiple comparisons. The Kruskal-Wallis test showed that the χ^2 value was 37.31 for the HAL group without thermocycling (Tc0-HAL group), 36.82 for the HAL group with 10,000 thermocycles (Tc10,000-HAL group), 40.22 for the ROC group without thermocycling (Tc0-ROC group) and 40.42 for the ROC group with 10,000 thermocycles (Tc10,000-ROC group). The p-value was less than 0.01 for all groups. Accordingly, the four groups were analyzed separately using the Steel-Dwass multiple comparisons. In addition, some binary conditions were selectively analyzed using the Mann-Whitney U test.

Shear bond strength

The shear bond strengths of the HAL group are presented in Table 2. The median bond strengths of the Tc0-HAL group varied from 2.3 to 27.8 MPa. Tc0-HAL-CP and AP showed the greatest bond strengths (category a). Tc0-HAL-UP resulted in the lowest bond strength (category c). The median bond strengths of the Tc10,000-HAL group varied from 0.3 to 29.8 MPa. Tc10,000-HAL-CP exhibited the greatest bond strength (category d). Tc10,000-HAL-UP and ES showed the lowest bond strengths (category f).

The shear bond strengths of the ROC group are presented in Table 3. The median bond strengths of the Tc0-ROC group varied from 2.4 to 28.7 MPa. Tc0-ROC-CP showed the greatest bond strength (category g). Tc0-ROC-UP resulted in the lowest bond strength (category j). The median bond strengths of the Tc10,000-ROC group varied from 0.5 to 30.3 MPa. Tc10,000-ROC-CP showed the greatest bond strength (category k), whereas Tc10,000-ROC-UP exhibited the lowest bond strength (category n).

Comparison of the pre- and post-thermocycling bond strengths revealed that the bond strengths of the seven groups differed significantly, except in the case of the ROC-CP group (Mann-Whitney U-test, Tables 2 and 3).

Selected binary conditions were compared using the Mann-Whitney U test (Table 4). Each of the three pairs (Tc10,000-HAL-AP *vs.* Tc10,000-ROC-ES, Tc10,000-HAL-AP *vs.* Tc10,000-ROC-AP, and Tc10,000-HAL-ES *vs.* Tc10,000-ROC-ES) differed significantly.

Failure mode analysis

The results of the failure mode analysis are summarized in Table 5. The Tc0-HAL group median cohesive failure ratio ranged from 6% (Tc0-HAL-UP) to 96% (Tc0-HAL-CP), and the Tc10,000-HAL group median cohesive failure ratio ranged from 0% (Tc10,000-HAL-UP) to 93% (Tc10,000-HAL-CP). The Tc0-ROC group median cohesive failure ratio ranged from 5% (Tc0-ROC-UP) to 89% (Tc0-ROC-CP), and the Tc10,000-HAL group median cohesive failure ratio ranged from 0% (Tc10,000-ROC-UP and AP) to 92% (Tc10,000-ROC-CP).

Electron microscopy observations

Figures 2a to 2c show the SEM images of the ground and after airborne-particle abrasion of the zirconia surfaces. The ground zirconia surface (Fig. 2a) exhibits scratches generated by the abrasive paper. The zirconia surfaces after HAL and ROC preparations (Figs. 2b and 2c) demonstrated roughened structures (Fig. 2a).

Figures 3a to 3d show typical debonded surfaces in the Tc10,000-HAL group. Tc10,000-HAL-UP (Fig. 3a) exhibited adhesive failure, similar to the zirconia surface after the HAL preparation (Fig. 2b). Tc10,000-HAL-CP (Fig. 3b) and Tc10,000-HAL-AP (Fig. 3c) showed

Table 5 Failure modes and cohesive failure ratio

Group	0 thermocycle				10,000 thermocycles			
	A	Cohesive failure ratio			A	Cohesive failure ratio		
		Mean (SD)	Median	IQR		Mean (SD)	Median	IQR
HAL-UP	2	6% (5)	6%	8	11	0% (0)	0%	0
HAL-CP	0	95% (3)	96%	6	0	93% (3)	93%	6
HAL-AP	0	94% (4)	95%	4	0	87% (4)	87%	8
HAL-ES	0	54% (6)	53%	10	5	2% (2)	2%	4
ROC-UP	2	6% (5)	5%	8	0	0% (0)	0%	0
ROC-CP	0	87% (7)	89%	11	11	90% (4)	92%	2
ROC-AP	0	15% (2)	15%	3	11	0% (0)	0%	0
ROC-ES	0	65% (9)	62%	14	0	33% (5)	32%	5

n=11; A, Adhesive failure at the resin-zirconia interface; SD, Standard deviation; IQR, interquartile range; Optical microscope: 57× magnification and an analyzing application

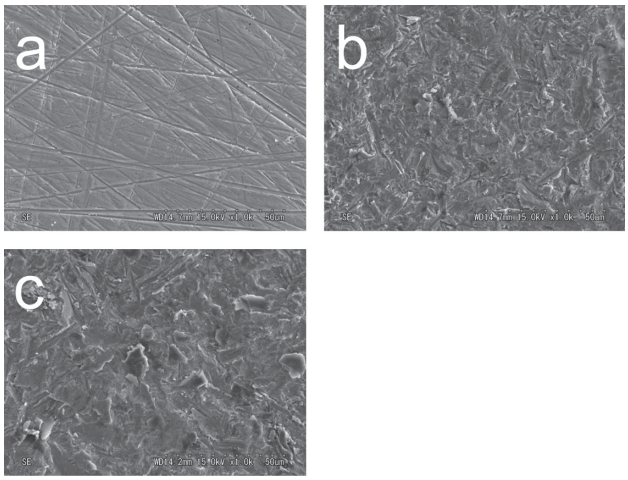

Fig. 2 Zirconia surfaces: (a) wet-ground with #800 SiC abrasive paper (control), (b) airborne-particle abraded with alumina (HAL), and (c) treated with the Rocatec system (ROC).

resin remnants on the zirconia surface, and exhibited a combination of adhesive and cohesive failure. Tc10,000-HAL-ES (Fig. 3d) exhibited adhesive failure, similar to the zirconia surface after HAL (Fig. 2b).

Figures 4a to 4d show representative debonded surfaces in the Tc10,000-ROC group. Tc10,000-ROC-UP (Fig. 4a) and Tc10,000-ROC-AP (Fig. 4c) exhibited adhesive failure, similar to the zirconia surface after ROC (Fig. 2c). Tc10,000-ROC-CP (Fig. 4b) and Tc10,000-ROC-ES (Fig. 4d) showed resin remnants on the zirconia surface and exhibited a combination of adhesive and cohesive failure. Resin remnants of Tc10,000-ROC-ES (Fig. 4d) were found to be smoother than that of Tc10,000-HAL-CP (Fig. 3b), Tc10,000-HAL-AP (Fig. 3c), and Tc10,000-ROC-CP (Fig. 4b).

Surface roughness

Surface roughness (*Ra* and *Sa*) values of the control, HAL, and ROC are presented in Table 6. The Kruskal-Wallis test (GraphPad Prism 6.0) and Steel-Dwass

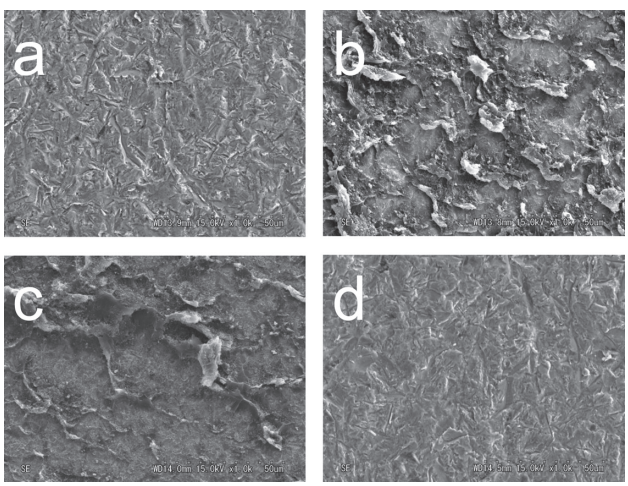

Fig. 3 Debonded surfaces of the alumina-blasted group (HAL, thermocycled): (a) unprimed, (b) primed with MDP-silane (CP), (c) primed with MDP (AP), and (d) primed with silane (ES).

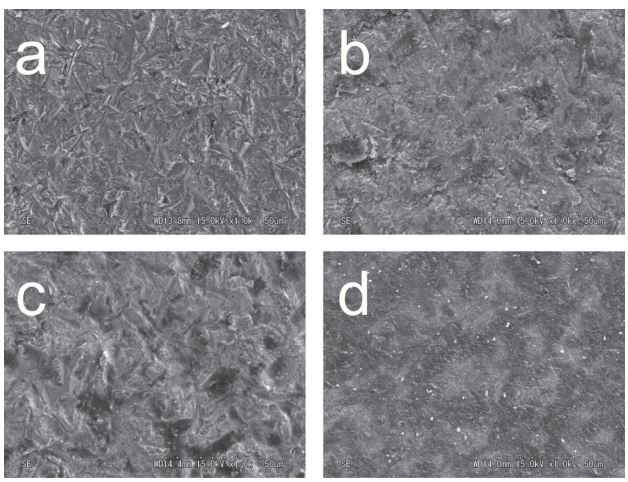

Fig. 4 Debonded surfaces of the Rocatec-treated group (ROC, thermocycled): (a) unprimed, (b) primed with MDP-silane (CP), (c) primed with MDP (AP), and (d) primed with silane (ES).

Table 6 Surface roughness (*Ra* and *Sa*)

	Surface roughness (*Ra*) (μm)			Surface roughness (*Sa*) (μm)		
	Mean (SD)	Median	IQR	Mean (SD)	Median	IQR
Control	0.23 (0.02)	0.23[o]	0.03	0.76 (0.03)	0.75[r]	0.06
HAL	0.49 (0.02)	0.49[p]	0.04	1.35 (0.07)	1.32[s]	0.11
ROC	1.26 (0.05)	1.26[q]	0.09	1.74 (0.06)	1.78[t]	0.10

n=5; SD, Standard deviation; IQR, interquartile range; Statistical category, Different letters indicate that the values are significantly different (Steel-Dwass test: $p<0.05$).

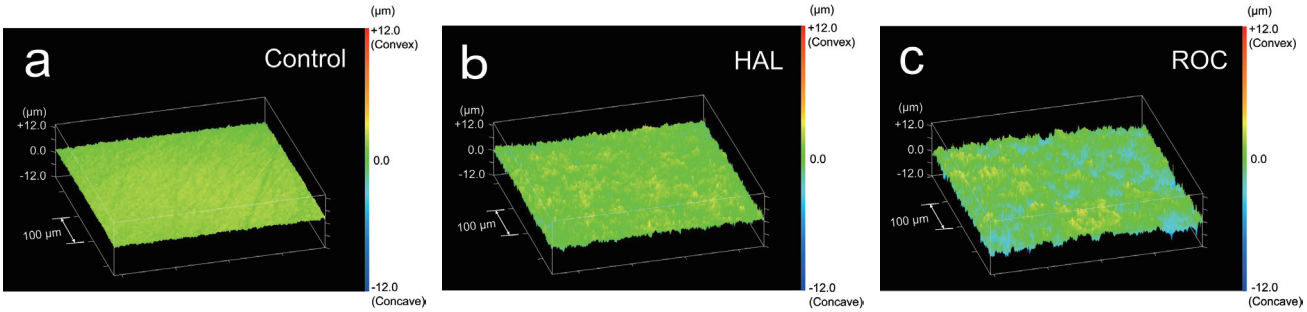

Fig. 5 The surface topographies of the zirconia specimens: (a) wet-ground with #800 SiC abrasive paper (control), (b) airborne-particle abraded with alumina (HAL), and (c) treated with the Rocatec system (ROC).

multiple comparisons (Kyplot 5.0) were applied to evaluate the impact of airborne-particle abrasion. The median *Ra* values were 0.23 μm for the control, 0.49 μm for HAL, and 1.26 μm for ROC. The *Ra* values differed significantly between the control, HAL, and ROC (categories o–q; $p<0.05$). The median *Sa* values were 0.75 μm for the control, 1.32 μm for HAL, and 1.78 μm for ROC. The *Sa* values differed significantly between the control, HAL, and ROC (categories r–t; $p<0.05$). ROC showed the highest surface roughness (categories q and t), whereas the control showed the lowest surface roughness (categories o and r).

The surface topographies of the specimens are shown in Fig. 5. The control showed the smoothest surface (Fig. 5a), whereas ROC showed the roughest surface (Fig. 5c). The control also demonstrated a trace ground with an 800-grit silicon carbide abrasive paper (Fig. 5a). Furthermore, HAL and ROC exhibited a concave-convex form by airborne-particle abrasion (Figs. 5b and 5c).

DISCUSSION

This study evaluated the shear bond strengths of a MMA-TBB self-polymerizing resin bonded to zirconia with mechanochemical surface preparations. A luting agent that did not contain any functional monomer was used to evaluate the impact of each functional monomer that was present in the primers. The results showed that only HAL-CP and ROC-CP groups maintained the stability of the bond strength after thermocycling. Thus, the null hypothesis was rejected.

The current study used phosphate MDP and MPTS as adhesive functional monomers. A number of studies reported that MDP is effective for bonding base metal alloys[19,20] and metal oxides[6-16,21]. CP and AP containing MDP showed higher bond strength values in the HAL group after 10,000 thermocycles compared to UP and ES that did not contain MDP.

MDP, one of the most hydrophobic phosphate monomers, enhanced the chemical bonding to the zirconia surface in agreement with previous studies[6-16]. Although the HAL-ES group showed a 21.0 MPa pre-thermocycling bond strength, the post-thermocycling bond strength was only 0.3 MPa. In addition, the post-thermocycling bond strengths to the HAL specimens did not significantly differ for the ES and UP groups. These results suggest that MPTS alone is not particularly effective as an adhesive functional monomer for zirconia bonding.

The shear bond strength of Tc10,000-HAL-AP (25.3 MPa) was significantly higher than that of Tc10,000-ROC-ES (13.5 MPa, Table 4). This suggests that the bonding between MDP and zirconia is more consistent and durable than the bonding between acid-catalyzed silane and silica-coated zirconia. Kern suggested that MDP contained primer on alumina blasted zirconia surface was first recommended compare to silica-coating following by silane primer on zirconia surface[22]. In addition, Tc10,000-ROC-CP (30.3 MPa) exhibited significantly higher values than Tc10,000-ROC-ES (13.5 MPa). These results suggest that MDP is more effective than some acid contained ES as a catalyst for silane coupling.

Ohlmann *et al.* evaluated the clinical performance of thirty zirconia based all-ceramic fixed dental prostheses using tribochemical silica-coating and a silane in combination with a MDP contained dual curing resin cement[23]. During the only 12 months observation period, a total of thirteen clinically relevant complications occurred during normal function despite a retentive inlay preparation design. Therefore, the combination of silica-coating and silane primer on zirconia surface do not achieve enough to stable bonding for clinical use. In this study, the cohesive failure ratio of Tc10,000-HAL-AP (87%) was higher values than that of Tc10,000-ROC-ES (32%). Furthermore, the results of SEM showed that resin remnants of Tc10,000-ROC-ES (Fig. 4d) were found to be smoother than that of Tc10,000-HAL-AP (Fig. 3c). These results demonstrated that HAL-AP was effective as surface preparation than ROC-ES. Moreover, deterioration at the adhesive interface treated silane primer is highly likely because of hydrolysis of the silane coupling layer[24]. Therefore, it concluded that silica-coating following by silane primer on zirconia surface do not produced durable bonding and could not be used clinically.

Shear bond strength of Tc10,000-HAL-AP (25.3 MPa) was significantly higher than that of Tc10,000-ROC-AP (1.7 MPa). In addition, bond strength of Tc10,000-ROC-ES (13.5 MPa) was significantly higher than that of Tc10,000-HAL-ES (0.3 MPa). Hallmann *et al.* reported that it is difficult for X-ray photoelectron spectroscopic analysis to detect zirconia element for the Rocatec-treated zirconia specimen surfaces, and they showed that the Rocatec-treated zirconia surface was coated with silica nano-particles[25]. It is understandable that the zirconia surface abraded with silica-coated alumina is coated with a silica layer and the modified surface is suitable for the priming silane monomer.

The surface roughness *Ra* and *Sa* of HAL and ROC were significantly higher than that of the ground specimens. These results indicate that both the single and the dual abrasion induce roughness of zirconia. The surface roughness *Ra* and *Sa* after the ROC preparation was significantly higher than that after the HAL preparation. However, the bond strength to the particle abraded zirconia of the unprimed control groups, UP-HAL and UP-ROC, were not significantly different. This indicates that the bond strength to zirconia of the MMA-TBB resin is substantially influenced by a combination of the specific functional monomer and surface modification rather than the material surface roughness.

ACKNOWLEDGMENTS

This work was supported in part by a Grant-in-Aid for Young Scientists (B) 26861657 (2014) from the Japan Society for the Promotion of Science (JSPS) and a grant from the Dental Research Center Nihon University School of Dentistry (2016).

CONFLICT OF INTEREST

The authors declare that they have no conflicts of interest regarded to this work.

REFERENCES

1) Piconi C, Maccauro G. Zirconia as a ceramic biomaterial. Biomaterials 1999; 20: 1-25.
2) Nordahl N, Vult von Steyern P, Larsson C. Fracture strength of ceramic monolithic crown systems of different thickness. J Oral Sci 2015; 57: 255-261.
3) Kato H, Matsumura H, Ide T, Atsuta M. Improved bonding of adhesive resin to sintered porcelain with the combination of acid etching and a two-liquid silane conditioner. J Oral Rehabil 2001; 28: 102-108.
4) Brentel AS, Ozcan M, Valandro LF, Alarca LG, Amaral R, Bottino MA. Microtensile bond strength of a resin cement to feldpathic ceramic after different etching and silanization regimens in dry and aged conditions. Dent Mater 2007; 23: 1323-1331.
5) Derand P, Derand T. Bond strength of luting cements to zirconium oxide ceramics. Int J Prosthodont 2000; 13: 131-135.
6) Kern M, Wegner SM. Bonding to zirconia ceramic: adhesion methods and their durability. Dent Mater 1998; 14: 64-71.
7) Attia A, Kern M. Long-term resin bonding to zirconia ceramic with a new universal primer. J Prosthet Dent 2011; 106: 319-327.
8) Koizumi H, Nakayama D, Komine F, Blatz MB, Matsumura H. Bonding of resin-based luting cements to zirconia with and without the use of ceramic priming agents. J Adhes Dent 2012; 14: 385-392.
9) Shin YJ, Shin Y, Yi YA, Kim J, Lee IB, Cho BH, Son HH, Seo DG. Evaluation of the shear bond strength of resin cement to Y-TZP ceramic after different surface treatments. Scanning 2014; 36: 479-486.
10) Chen C, Xie H, Song X, Burrow MF, Chen G, Zhang F. Evaluation of a commercial primer for bonding of zirconia to two different resin composite cements. J Adhes Dent 2014; 16: 169-176.
11) Pereira Lde L, Campos F, Dal Piva AM, Gondim LD, Souza RO, Ozcan M. Can application of universal primers alone be a substitute for airborne-particle abrasion to improve adhesion of resin cement to zirconia? J Adhes Dent 2015; 17: 169-174.
12) Yi YA, Ahn JS, Park YJ, Jun SH, Lee IB, Cho BH, Son HH, Seo DG. The effect of sandblasting and different primers on shear bond strength between yttria-tetragonal zirconia polycrystal ceramic and a self-adhesive resin cement. Oper Dent 2015; 40: 63-71.
13) da Silva EM, Miragaya L, Sabrosa CE, Maia LC. Stability of the bond between two resin cements and an yttria-stabilized zirconia ceramic after six months of aging in water. J Prosthet Dent 2014; 112: 568-575.
14) Nakayama D, Koizumi H, Komine F, Blatz MB, Tanoue N, Matsumura H. Adhesive bonding of zirconia with single-liquid acidic primers and a tri-*n*-butylborane initiated acrylic resin. J Adhes Dent 2010; 12: 305-310.
15) Oba Y, Koizumi H, Nakayama D, Ishii T, Akazawa N, Matsumura H. Effect of silane and phosphate primers on the adhesive performance of a tri-*n*-butylborane initiated luting agent bonded to zirconia. Dent Mater J 2014; 33: 226-232.
16) Kim JH, Chae SY, Lee Y, Han GJ, Cho BH. Effects of multipurpose, universal adhesives on resin bonding to zirconia ceramic. Oper Dent 2015; 40: 55-62.
17) Aboushelib MN, Kleverlaan CJ, Feilzer AJ. Selective infiltration-etching technique for a strong and durable bond of resin cements to zirconia-based materials. J Prosthet Dent 2007; 98: 379-388.
18) Jevnikar P, Krnel K, Kocjan A, Funduk N, Kosmac T. The effect of nano-structured alumina coating on resin-bond strength to zirconia ceramics. Dent Mater 2010; 26: 688-696.
19) Ishii T, Koizumi H, Tanoue N, Naito K, Yamashita M, Matsumura H. Effect of alumina air-abrasion on mechanical bonding between an acrylic resin and casting alloys. J Oral Sci 2009; 51: 161-166.
20) Masuno T, Koizumi H, Ishikawa Y, Nakayama D, Yoneyama T, Matsumura H. Effect of acidic monomers on bonding to SUS XM27 stainless steel, iron, and chromium with a tri-*n*-butylborane-initiated acrylic resin. J Adhes Dent 2011; 13: 163-169.
21) Yamada K, Koizumi H, Kawamoto Y, Ishikawa Y, Matsumura H, Tanoue N. Effect of single-liquid priming agents on adhesive bonding to aluminum oxide of a methacrylic resin. Dent Mater J 2007; 26: 642-646.
22) Kern M. Resin bonding to oxide ceramics for dental restorations. J Adhes Sci Technol 2009; 23: 1097-1111.
23) Ohlmann B, Rammelsberg P, Schmitter M, Schwarz S, Gabbert O. All-ceramic inlay-retained fixed partial dentures: preliminary results from a clinical study. J Dent 2008; 36: 692-696.
24) Nihei T. Dental applications for silane coupling agents. J Oral Sci 2016; 58: 151-155.
25) Hallmann L, Ulmer P, Reusser E, Hammerle CH. Surface characterization of dental Y-TZP ceramic after air abrasion treatment. J Dent 2012; 40: 723-735.